International Journal of Computer Vision 49(1), 23–37, 2002

Epipolar Geometry for Central Catadioptric Cameras*

TOMÁŠ SVOBODA† AND TOMÁŠ PAJDLA
Center for Machine Perception, Department of Cybernetics, Faculty of Electrical Engineering, Czech Technical University, Karlovo nám. 13, CZ 121 35 Prague, Czech Republic
svoboda@cmp.felk.cvut.cz
pajdla@cmp.felk.cvut.cz

Abstract. Central catadioptric cameras are cameras which combine lenses and mirrors to capture a very wide field of view with a central projection. In this paper we extend the classical epipolar geometry of perspective cameras to all central catadioptric cameras. Epipolar geometry is formulated as the geometry of corresponding rays in a three-dimensional space. Using the model of image formation of central catadioptric cameras, the constraint on corresponding image points is then derived. It is shown that the corresponding points lie on epipolar conics. In addition, the shape of the conics for all types of central catadioptric cameras is classified. Finally, the theory is verified by experiments with real central catadioptric cameras.

Keywords: epipolar geometry, panoramic vision, omnidirectional vision, catadioptric camera

1. Introduction

Epipolar geometry (Faugeras, 1993) describes the relationship between positions of corresponding points in a pair of images. It can be established from a few image correspondences and is used to: simplify the search for more correspondences, compute the displacement between the cameras, and reconstruct the scene.

Recently, a number of catadioptric camera designs have appeared (Yagi, 1999; Svoboda and Pajdla, 2000). The catadioptric cameras combine lenses and mirrors to capture a wide, often panoramic, field of view. It is advantageous to capture a wide field of view for the following three reasons. First, a wide field of view eases the search for correspondences as the corresponding points do not disappear from the images very often. Second, a wide field of view helps to stabilize egomotion estimation algorithms, so that the rotation of the camera can be easily distinguished from its translation (Brodsky et al., 1998). Last but not least, almost complete reconstructions of a surrounding scene can be obtained from two panoramic images.

This paper will concentrate on catadioptric cameras which consist of a single conventional perspective camera looking at a single curved mirror. We do not consider planar mirrors because the geometry is exactly the same as if we use the mirror image of a conventional camera. Moreover, we will assume that the camera and the mirror are arranged in a configuration to assure that the whole catadioptric camera has a *single effective viewpoint*. Let us call such cameras *central catadioptric cameras*.

Baker and Nayar (1999) have proved that among all curved mirrors, only the quadric mirrors shown in Fig. 1 can be placed in a configuration with a perspective camera, so that all the rays reflected from the mirror intersect at a single effective viewpoint other than the center of the perspective camera. If the center of the conventional perspective camera is placed into one focal point of the mirror, then the reflected rays

*This research was supported by the Czech Ministry of Education under the grant VS96049 and MSMT Kontakt 2001/09, by the Grant Agency of the Czech Republic under the grant GACR 102/01/0971, by the Research Programme J04/98:212300013 Decision and control for industry, and by EU Fifth Framework Programme project Omniviews No. 1999-29017.
†Present address: Swiss Federal Institute of Technology, Zürich, Switzerland.

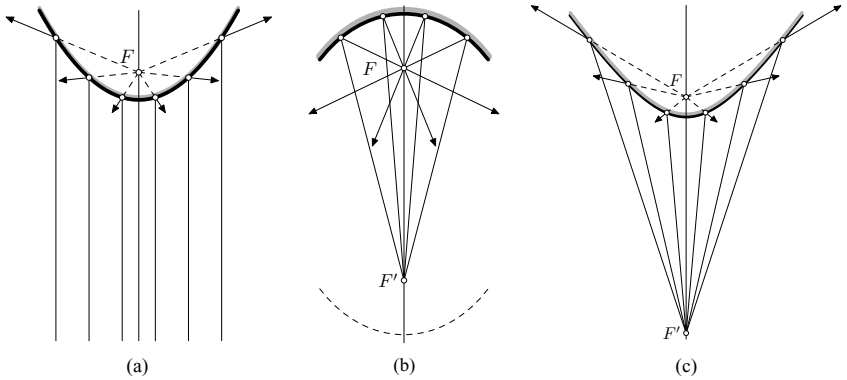

Figure 1. (a) Parabolic, (b) elliptic, and (c) hyperbolic mirrors allow a central projection by reflected rays.

will intersect at the other focal point of the mirror. The elliptic and hyperbolic mirrors, as seen in Fig. 1(b) and (c), have finite focal points F, F' respectively. They are imaged by perspective cameras from the point F'. The parabolic mirror in Fig. 1(a) has the focal point F' at infinity. It is imaged by an orthographic camera. It should be noted that this orthographic camera is nothing other than a perspective camera with its center placed at the focal point F' which is at infinity.

It is not necessary to consider central catadioptric cameras with more quadric mirrors arranged in a chain. By a chain we mean an arrangement of the mirrors in which the second focal point of the first mirror would coincide with the first focal point of the second mirror and so on. It has been shown (Nayar and Peri, 1999) that such a *folded system* of quadric mirrors is geometrically equivalent to a system with a single quadric mirror.

Epipolar geometry is a property of cameras with a central projection. It is natural to define the epipolar geometry of central catadioptric cameras as the epipolar geometry associated with the effective viewpoints of the complete catadioptric systems. Thus, the fundamental epipolar constraint is the same for conventional perspective as that for central catadioptric cameras if it is formulated in terms of rays which emanate from the effective viewpoints. In both cases, all rays from one camera, which may correspond to a ray from the other camera, have to lie in an epipolar plane. Differences appear when the constraint is formulated in terms of pixel coordinates of the corresponding image points. Then, the conventional epipolar constraint is replaced by a more complex one and the conventional epipolar lines are replaced by epipolar curves. It is the main goal of this work to express the epipolar constraint and the epipolar curves in image coordinates.

The paper is organized as follows. First, previous work is reviewed in Section 2. Then, in Section 3, the imaging models for central catadioptric cameras with hyperbolic, elliptic, and parabolic mirrors are derived. In Section 4, epipolar geometry for these cameras is introduced, the epipolar constraint is formulated using the coordinates of corresponding image points, and the shape of epipolar curves in images is discussed. Finally, the theory is verified by experiments with real cameras in Section 5.

2. Previous Work

Many designs of panoramic catadioptric cameras appeared in the last decade in computer vision. A comprehensive survey can be found in Yagi (1999) or in Svoboda and Pajdla (2000). Some other works utilizing curved mirrors have also appeared in robotics for navigating mobile robots, see e.g. Yamazawa et al. (1995). Here, we focus on works related to epipolar geometry of catadioptric cameras which have single effective viewpoint.

Central catadioptric cameras have a long history. In 1637 René Descartes presented an analysis of the geometry of mirrors and lenses in *Discours de la Methode* (Descartes and Smith, 1954). He showed that refractive as well as reflective 'ovals' (conical lenses and mirrors) focus light into a single point if they are illuminated from another properly chosen point (Hecht, 1975). Recently, the characterization of curved mirrors preserving a single viewpoint was reformulated into the modern language of the computer vision community by Baker and Nayar (1999). Geometrical properties and optics of folded catadioptric cameras were studied by Nayar and Peri (1999).

A few works related to epipolar geometry of catadioptric cameras have also been recently developed. Southwell et al. (1996) proposed a camera-mirrors system consisting of a double lobed mirror, i.e. of two mirrors in a fixed relative position, observed by one camera. Such a system has a special epipolar geometry when epipolar curves are radial lines. Nene and Nayar (1998) studied the epipolar geometry for the limited case of a pure rotation of a hyperbolic mirror around the center of a conventional camera or, equivalently, for the case of a pure translation of a parabolic mirror with respect to an orthographic camera. Gluckman and Nayar (1998) estimated the ego-motion of the omnidirectional cameras by an optical flow algorithm. Svoboda et al. (1998b) studied the stability of the ego-motion estimation from corresponding points in images from a central catadioptric camera with a hyperbolic mirror. All of the above works used some facts which follows from the general analysis of epipolar geometry of central catadioptric cameras. However, they were restricted to dealing with special relative positions of the cameras (Southwell et al., 1996; Nene and Nayar, 1998) or studying the behavior of ego-motion algorithms (Gluckman and Nayar, 1998; Svoboda et al., 1998b) and did not address the general problem of formulating epipolar geometry.

The concept of epipolar geometry for central catadioptric cameras in its full generality was, for the first time, presented in our previous conference paper (Svoboda et al., 1998a), where the cameras with hyperbolic mirrors were studied. Our work (Pajdla et al., 2001) has added an analysis of cameras with parabolic mirrors, a general classification of omnidirectional cameras, and an analysis of epipolar geometry estimation from image correspondences. This work generalizes and finalizes our previous work on the epipolar geometry of panoramic catadioptric cameras by providing a general formulation of epipolar geometry for all central catadioptric cameras.

3. Camera Models

In this section, we study the geometry of image formation for central catadioptric cameras. Points in a 3D space are represented by upper case letters, such as X or by bold upper case letters, such as $\mathbf{X}$, if we refer to their coordinates. Homogeneous vectors corresponding to image points or rays are represented by bold lower case letters, such as $\mathbf{x}$. The symbol $\|\mathbf{x}\|$ stands for the length of a vector $\mathbf{x}$.

By the conventional camera model we understand the relationship between the coordinates of a 3D point $\mathbf{X}$ and its projection, $\mathbf{u}$, in the image

$$\mathbf{x} = [R, -R\mathbf{t}]\mathbf{X}, \tag{1}$$

$$\mathbf{u} = K\frac{1}{\alpha}\mathbf{x} \quad \text{where } \alpha \in \mathsf{R},\ \alpha \neq 0, \tag{2}$$

where $\mathbf{X} = [X, Y, Z, 1]^T$ is a 4-vector representing a 3D point, $\mathbf{t}$ is the position of the camera center, and R is the rotation between the camera and a world coordinate system. Matrix K is a 3×3 upper triangular camera calibration matrix with $K_{33} = 1$. Vector $\mathbf{x} = [x, y, z]^T$ represents point coordinates in the coordinate system of the camera. The scale α equals the z coordinate of $\mathbf{x}$. Vector $\mathbf{u} = [u, v, 1]^T$ represents the homogeneous pixel image coordinates which are measured in an image. See Faugeras (1993) and Hartley and Zisserman (2000) for more details about the model of a conventional camera.

All coordinates are expressed in the coordinate system placed in the single effective viewpoint denoted by F in Fig. 1, with the z axis aligned with the axis of the mirror. The use of a different coordinate system will be stated explicitly.

Let us derive a general imaging model for a central catadioptric camera and then discuss the individual mirrors. Quadric surfaces can be expressed by the general equation

$$\mathbf{X}^T Q \mathbf{X} = 0, \tag{3}$$

where Q is a 4×4 matrix that varies depending on the type of the quadric (Semple and Kneebone, 1998). A space point $\mathbf{X}$ is projected by a central projection to the point $\mathbf{x}$ on the mirror surface as

$$\mathbf{x} = \lambda[R_m, -R_m\mathbf{t}_m]\mathbf{X}, \quad \lambda \in \mathsf{R}, \quad \lambda \neq 0, \tag{4}$$

where the subscript m denotes the transformation between a space coordinate system and the coordinate system centered at the mirror focal point F. Scale λ is discussed further in the text. The point on the mirror surface is then projected to the image plane of a conventional camera

$$\mathbf{u} = K\frac{1}{\alpha}[R_c, -R_c\mathbf{t}_c]\begin{bmatrix}\mathbf{x}\\ 1\end{bmatrix}, \tag{5}$$

where the subscript c denotes the transformation between the mirror and the camera coordinate system.

The scale α normalizes the transformed vector to normalized homogeneous coordinates and K is a camera calibration matrix. The scale factor α is equal to the z coordinate of the vector

$$[R_c, -R_c\mathbf{t}_c]\begin{bmatrix}\mathbf{x}\\1\end{bmatrix}.$$

We see that the imaging model of a central catadioptric camera is a composition of two central projections. The scale λ from (4) can be computed by solving

$$\begin{bmatrix}\lambda[R_m, -R_m\mathbf{t}_m]\mathbf{X}\\1\end{bmatrix}^T Q\begin{bmatrix}\lambda[R_m, -R_m\mathbf{t}_m]\mathbf{X}\\1\end{bmatrix} = 0. \tag{6}$$

This is a quadratic equation with respect to λ.

The general imaging model, just described, can be used for any camera combining a quadric mirror and a conventional camera in such a way that the rays reflected from the mirror all intersect at one focal point of the mirror. In the next three sections we will work out imaging models for catadioptric cameras with parabolic, hyperbolic, and elliptic mirrors.

3.1. Parabolic Mirror and Orthographic Camera

The simplest central catadioptric camera is composed of a convex parabolic mirror and an orthographic camera. The matrix Q from (3) for a paraboloid of revolution is

$$Q_p = \begin{bmatrix}\frac{-1}{b^2} & 0 & 0 & 0\\ 0 & \frac{-1}{b^2} & 0 & 0\\ 0 & 0 & 0 & \frac{1}{b}\\ 0 & 0 & \frac{1}{b} & 1\end{bmatrix}, \tag{7}$$

where b is twice the distance from the vertex[1] to the focal point and is called the mirror parameter. The general model (5) is simplified here because the scale $1/\alpha$ is not considered, and the translation $\mathbf{t}_c$ makes no sense since the camera center is at infinity. The axis of the orthographic camera has to coincide with the axis of the mirror, otherwise the reflected rays will not intersect at the focal point F.

Let us find the scale λ from (4). Substituting (7) into (6) gives us a quadratic equation in λ

$$\lambda^2(-x^2 - y^2) + \lambda(2bz) + b^2 = 0,$$

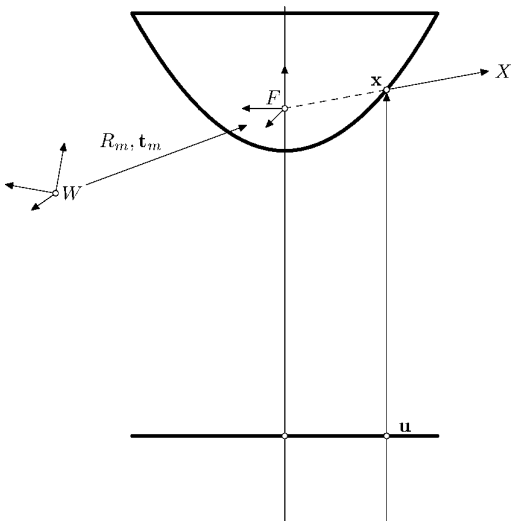

Figure 2. An orthographic camera with a parabolic mirror assembled so that the rays of the conventional camera are parallel to the mirror symmetry axis. The reflected rays intersect in F.

where

$$[x, y, z]^T = [R_m, -R_m\mathbf{t}_m]\mathbf{X}.$$

Two solutions exist except for the case when the point X lies on the mirror axis. Then, only one solution exists. Assuming that the point X is not on the mirror axis, the intersection point between F and X, see Fig. 2, is the one that is relevant for our purpose. Thus it holds that

$$\lambda = \frac{b(z + \sqrt{x^2 + y^2 + z^2})}{x^2 + y^2}. \tag{8}$$

For a point on the mirror axis it holds $\lambda = -b/2z$. Once λ is determined, the complete projection from $\mathbf{X}$ to pixel coordinates $\mathbf{u}$ can be written as

$$\mathbf{u} = KR_c\begin{bmatrix}\lambda\begin{bmatrix}1 & 0 & 0\\ 0 & 1 & 0\end{bmatrix}[R_m, -R_m\mathbf{t}_m]\mathbf{X}\\1\end{bmatrix}, \quad \text{where}$$

$$R_c = \begin{bmatrix}r_{11} & r_{12} & 0\\ r_{21} & r_{22} & 0\\ 0 & 0 & 1\end{bmatrix}. \tag{9}$$

Since the projection rays are parallel, the transformation, which has to be composed with the projection, is an affine transformation and therefore the product KR_c

must be an affine transformation. With a triangular K, the transformation is affine only if the rotation R_c is in the form given by (9).

If a projected point $\mathbf{u}$ is known, the point on the mirror surface can be computed directly as

$$\mathbf{x} = \begin{bmatrix} x \\ y \\ \frac{x^2+y^2}{2b} - \frac{b}{2} \end{bmatrix}, \quad \text{where} \quad \begin{bmatrix} x \\ y \\ 1 \end{bmatrix} = R_c^T K^{-1}\mathbf{u}. \tag{10}$$

There are six external calibration parameters (three for $\mathbf{t}_m$ and three for R_m) and seven internal calibration parameters (one for the mirror, one for R_c, and five for K).

3.2. Hyperbolic Mirror and Perspective Camera

The matrix Q from (3) for a hyperbolic mirror is

$$Q_h = \begin{bmatrix} -\frac{1}{b^2} & 0 & 0 & 0 \\ 0 & -\frac{1}{b^2} & 0 & 0 \\ 0 & 0 & \frac{1}{a^2} & \frac{e}{a^2} \\ 0 & 0 & \frac{e}{a^2} & \frac{b^2}{a^2} \end{bmatrix}, \tag{11}$$

where a, b are mirror parameters and the focal length is $e = \sqrt{a^2 + b^2}$. The hyperbolic mirror is one part of a two-sheet hyperboloid of revolution (Hazewinkel, 1995). Suppose that the projection center C of a conventional camera is placed at the focal point of this quadric, $F' = C$, see Fig. 3. Then, all the rays going from (or into) the center of projection C intersect at the second focal point F after being reflected from the mirror. We derive the imaging model assuming that the perspective camera is properly placed, or equivalently, that all of the rays reflected from the mirror intersect in F. Substituting (11) into (6) yields a quadratic equation in λ

$$\lambda^2(b^2z^2 - a^2x^2 - a^2y^2) + \lambda\,(2b^2ez) + b^4 = 0,$$

where

$$\mathbf{v} = [x, y, z]^T = [R_m, -R_m\mathbf{t}_m]\mathbf{X},$$

with the solution

$$\lambda_{1,2} = \frac{b^2(-ze \pm a\sqrt{\|\mathbf{v}\|})}{z^2b^2 - x^2a^2 - y^2a^2}. \tag{12}$$

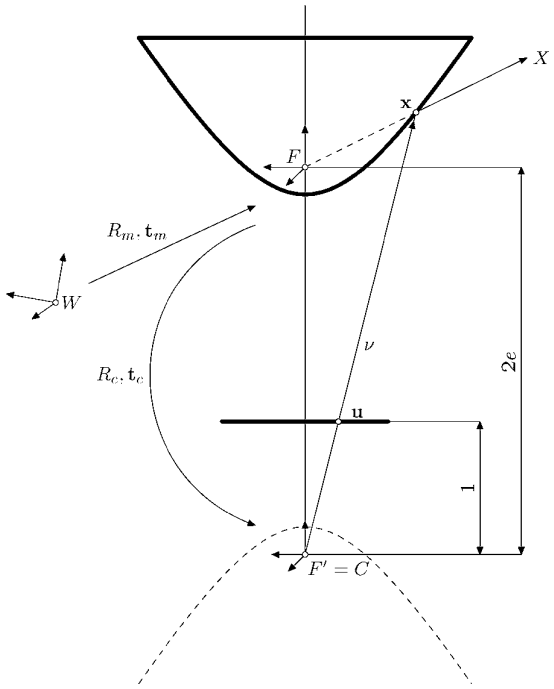

Figure 3. A conventional camera assembled with a hyperbolic mirror so that the camera center C coincides with the focal point of the mirror F'. The rays reflected from the mirror intersect in F.

It can be verified that $\lambda_{1,2}$ are real and never equal to zero for $X \neq F$. Let us choose the λ that corresponds to the intersection which lies between the points F and X. The signs of $\lambda_{1,2}$ depend on the position of the point X with respect to the mirror. There are three combinations of the signs (as $\lambda_1 > \lambda_2$) which partition the space of X into three areas, see Fig. 4. First, the points from the area $\pi_{-,-}$ for which $\lambda_{1,2} < 0$ cannot be seen because they are inside of the mirror. Second, for $X \in \pi_{+,+}$, the intersection with the sheet which corresponds to the mirror is given by $\lambda = \min(\lambda_{1,2})$. Finally, for $X \in \pi_{+,-}$, the correct intersection is given by $\lambda = \max(\lambda_{1,2})$ to obtain a point between F and X. Once the correct λ is determined, the coordinates of the point $\mathbf{x}$ on the mirror are computed by using (4).

Vector $\mathbf{x}$ is expressed in the coordinate system centered at C as

$$\mathbf{x}_c = R_c(\mathbf{x} - \mathbf{t}_c), \tag{13}$$

where R_c stands for the rotation and $\mathbf{t}_c$ for the translation between the systems F and C. The translation $\mathbf{t}_c$

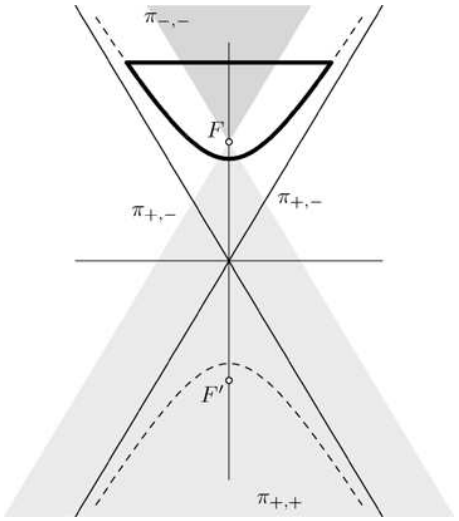

Figure 4. The signs of $\lambda_{1,2}$ partition the space into three areas.

cannot be arbitrary because the conventional camera center C has to coincide with F' in order to have a projection center in F. Thus the translation must be $\mathbf{t}_c = [0, 0, -2e]^T$. The rotation R_c, on the other hand, can be arbitrary as long as the mirror is seen by the camera. Although this might look suspicious, note that only the coincidence of the camera center with the focal point of the hyperboloid is required. The coordinate system of the camera can be arbitrarily rotated. However, the z-axis of the camera coordinate system is usually aligned with the camera's optical axis. Figure 3 shows the most frequent situation when R_c is the identity.

Point $\mathbf{x}_c$ is projected into the image point with pixel coordinates

$$\mathbf{u} = K\frac{1}{z_c}\mathbf{x}_c, \quad \text{with } \mathbf{x}_c = [x_c, y_c, z_c]^T. \tag{14}$$

Putting (14), (13), and (4) together, the complete model of a central catadioptric camera can be concisely rewritten as

$$\mathbf{u} = K\frac{1}{z_c}R_c(\lambda[R_m, -R_m\mathbf{t}_m]\mathbf{X} - \mathbf{t}_c), \tag{15}$$

where λ is one of $\lambda_{1,2}$ from (12) and z_c is defined by (14) and (13).

Sixteen calibration parameters appear in (15). There are 6 free external calibration parameters (three for $\mathbf{t}_m$ and three for R_m) and 10 free internal parameters (two for the mirror (a, b), three for the rotation matrix R_c, and five intrinsic parameters of the perspective camera in K).

Let us show how $\mathbf{x}$ is obtained from $\mathbf{u}$. The line ν, see Fig. 3, going from the center C in the direction $\mathbf{u}$, consists of points

$$\nu = \left\{ \mathbf{w} \mid \mathbf{w} = \lambda \begin{bmatrix} r \\ s \\ t \end{bmatrix} - \begin{bmatrix} 0 \\ 0 \\ 2e \end{bmatrix} = \lambda\mathbf{v} + \mathbf{t}_c \right.$$
$$\left. = \lambda R_c^T K^{-1}\mathbf{u} + \mathbf{t}_c,\ \lambda \in \mathsf{R} \right\}. \tag{16}$$

Substituting $\mathbf{w}$ from (16) into the mirror equation (11) and (3) yields

$$\lambda^2(b^2t^2 - a^2r^2 - a^2s^2) - \lambda(2b^2et) + b^4 = 0.$$

Solving this quadratic equation gives

$$\lambda_{1,2} = \frac{b^2(et \pm a\|\mathbf{v}\|)}{b^2t^2 - a^2r^2 - a^2s^2}. \tag{17}$$

The decision of which λ corresponds to the correct intersection is straightforward. Going from C in direction $\mathbf{u}$, we are interested in the intersection which is farther from the point C, hence $\lambda = \lambda_1$. The complete transformation from $\mathbf{u}$ to $\mathbf{x}$ can be concisely written as

$$\mathbf{x} = \mathcal{F}_h\big(R_c^T K^{-1}\mathbf{u}\big)R_c^T K^{-1}\mathbf{u} + \mathbf{t}_c, \tag{18}$$

with

$$\mathcal{F}_h(\mathbf{v}) = \frac{b^2(et + a\|\mathbf{v}\|)}{b^2t - a^2r^2 - a^2s^2}, \quad \text{where}$$
$$\mathbf{v} = [r, s, t]^T = R_c^T K^{-1}\mathbf{u}. \tag{19}$$

3.3. Elliptic Mirror and Perspective Camera

The elliptic mirror is a part of an ellipsoid of revolution (Hazewinkel, 1995). The matrix Q from (3) for an elliptic mirror is

$$Q_e = \begin{bmatrix} \frac{1}{b^2} & 0 & 0 & 0 \\ 0 & \frac{1}{b^2} & 0 & 0 \\ 0 & 0 & \frac{1}{a^2} & \frac{e}{a^2} \\ 0 & 0 & \frac{e}{a^2} & -\frac{b^2}{a^2} \end{bmatrix}, \tag{20}$$

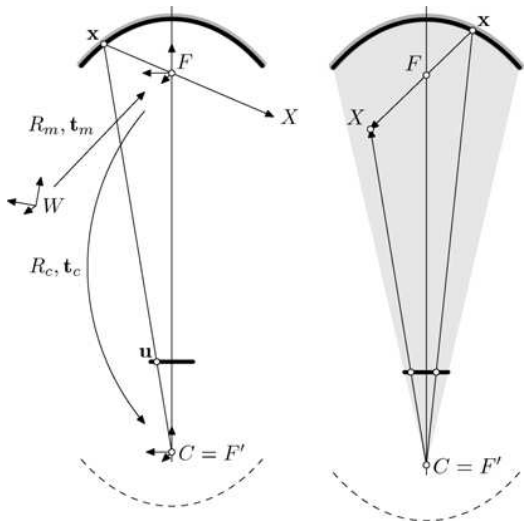

Figure 5. Left: A concave elliptic mirror with a perspective camera placed at the focal point F'. Right: Forbidden zone for space points. A space point X is assumed to lie outside shaded area otherwise it would be imaged twice to the projection plane.

where a, b are mirror parameters and the focal length is $e = \sqrt{a^2 - b^2}$. Suppose that the camera projection center of a perspective camera is placed at the focal point of this quadric, $F' = C$, as shown in Fig. 5. Then, all reflected rays intersect at the second focal point F. Substituting (20) into (6) gives us a quadratic equation in λ with the solution

$$\lambda_{1,2} = \frac{b^2(-ze \pm a\sqrt{\|\mathbf{v}\|})}{z^2b^2 + x^2a^2 + y^2a^2}, \tag{21}$$

where $\mathbf{v} = [x, y, z]^T = [R_m, -R_m\mathbf{t}_m]\mathbf{X}$. The decision of which λ to choose in (21) is made by the following reasoning. We suppose that a point X lies outside the shaded area shown in Fig. 5. Otherwise, it would be imaged twice in the projection plane. The twofold projection of the point could be useful in some applications, however, this is not considered here.[2] Further transformations are the same as those for the hyperbolic mirror. The complete model, of how a space point is projected to pixel coordinates in the camera is the same as in (15) with $\lambda = \lambda_2$ from (21). The number of calibration parameters is the same, 6 and 10 for external and internal parameters, respectively.

When pixel coordinates of a projected point $\mathbf{u}$ are known then the coordinates of the point on the mirror $\mathbf{x}$ are computed similarly as those for the hyperbolic mirror given by (18) where $\mathcal{F}_h$ is substituted for $\mathcal{F}_e$

$$\mathcal{F}_e(\mathbf{v}) = \frac{b^2(et + a\|\mathbf{v}\|)}{b^2t + a^2r^2 + a^2s^2}, \quad \text{where}$$
$$\mathbf{v} = [r, s, t]^T = R_c^T K^{-1}\mathbf{u}. \tag{22}$$

4. Epipolar Geometry

Epipolar geometry describes a geometric relationship between the positions of the corresponding points in two images acquired by central cameras (Faugeras, 1993). Since the epipolar geometry is a property of central projection cameras, it also exists for central catadioptric cameras.

Let us study what the epipolar curves look like for central catadioptric cameras with quadric mirrors. Let the translation $\mathbf{t}$ and the rotation R relate the coordinate systems F_1 and F_2, see Fig. 6. Let the projections of a 3D point X onto the mirrors be denoted as $\mathbf{x}_1$ and $\mathbf{x}_2$. The coplanarity of vectors $\mathbf{x}_1$, $\mathbf{x}_2$, and $\mathbf{t} = [t_x, t_y, t_z]^T$ can be expressed in the coordinate system F_2 as

$$\mathbf{x}_2^T R(\mathbf{t} \times \mathbf{x}_1) = 0, \tag{23}$$

where $\times$ denotes the vector product. Introducing an antisymmetric matrix S

$$S = \begin{bmatrix} 0 & -t_z & t_y \\ t_z & 0 & -t_x \\ -t_y & t_x & 0, \end{bmatrix}, \tag{24}$$

the coplanarity constraint (23) is rewritten in the matrix form as

$$\mathbf{x}_2^T E\mathbf{x}_1 = 0, \tag{25}$$

where

$$E = RS \tag{26}$$

is the essential matrix (Hartley and Zisserman, 2000). Vectors $\mathbf{x}_1$, $\mathbf{x}_2$, and $\mathbf{t}$ form the *epipolar plane* π. The epipolar plane π intersects the mirrors in intersection conics that are projected by a central projection into conics in image planes. To each point $\mathbf{u}_1$ in one image, an epipolar conic is uniquely assigned in the other image. Expressed algebraically, it provides us with the *fundamental constraint* on the corresponding points in

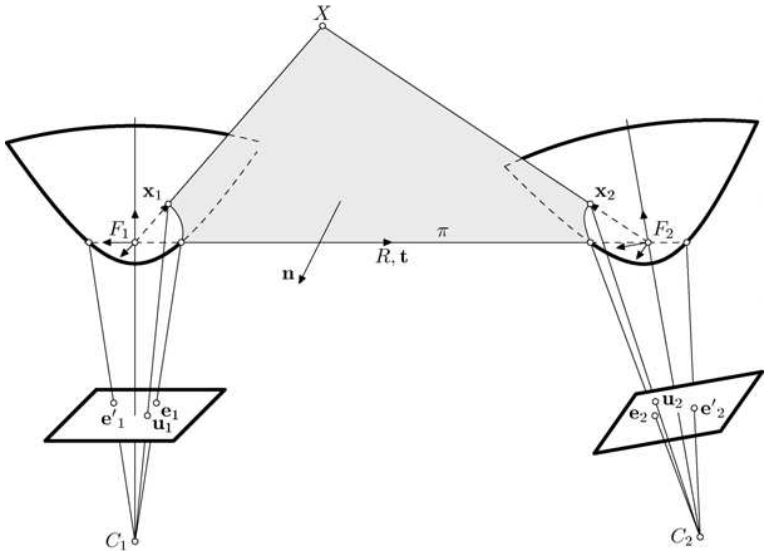

Figure 6. The epipolar geometry of two central catadioptric cameras with hyperbolic mirrors.

two central catadioptric images

$$\mathbf{u}_2^T A_2(E, \mathbf{u}_1)\, \mathbf{u}_2 = 0. \tag{27}$$

In a general case, the matrix $A_2(E, \mathbf{u}_1)$ is a nonlinear function of the essential matrix E, the point $\mathbf{u}_1$, and the calibration parameters of the central catadioptric camera.

The shape of the conics, i.e. if they are lines, circles, ellipses, parabolas, or hyperbolas, depends on the shape of the mirrors, the relative position of the cameras, and on which point is considered in the image. It holds true that there is at least one line among all epipolar conics in each image. It is the line which corresponds to the epipolar plane containing the axis of the mirror. There exists a pair of corresponding epipolar lines if the motion is a proper translation. Moreover, if the translation occurs along the axis of the mirror, all epipolar curves become lines. It is clear that the epipolar curves form a one-parameter family of conics which is parameterized by the angle of rotation of the epipolar plane around the vector $\mathbf{t}$.

All epipolar conics pass through two points which are the images of the intersections of the mirrors with the line F_1F_2. These points are two epipoles in two cameras, denoted $\mathbf{e}_1$ and $\mathbf{e}'_1$, respectively $\mathbf{e}_2$ and $\mathbf{e}'_2$, in Fig. 6. The epipoles can degenerate into a double epipole, if the camera is translated along the symmetry axis of the mirror.

In the next three sections we analyze the epipolar geometry of central catadioptric cameras with one mirror. We derive the fundamental equation of epipolar geometry and the equations for epipolar conics in image coordinates. We start with the most general case, a perspective camera with a hyperbolic mirror.

4.1. Hyperbolic Mirror

Let us derive $A_2(E, \mathbf{u}_1)$ from Eq. (27) for the central catadioptric camera with a hyperbolic mirror. In order to do so, we first find the equation of an orthographic projection of the intersection conic from the mirror to the xy plane of the coordinate system F_2. The intersection conic on the mirror is obtained by intersecting the epipolar plane with the mirror, see Fig. 6. The equation of the conic, expressed in an orthographic projection to the xy plane, is

$$\bar{\mathbf{x}}_2^T A_{\bar{\mathbf{x}}_2} \bar{\mathbf{x}}_2 = 0, \tag{28}$$

where

$$\bar{\mathbf{x}}_2 = [x, y, 1]^T \quad \text{and} \quad \mathbf{x}_2 = [x, y, z]^T. \tag{29}$$

Let us find $A_{\bar{\mathbf{x}}_2}$. The focal point of the first mirror F_1, the vector $\mathbf{x}_1$, and the vector $\mathbf{t}$ define the epipolar plane π. The normal vector of the plane π, expressed in the

coordinate system F_1, is

$$\mathbf{n}_1 = \mathbf{t} \times \mathbf{x}_1. \tag{30}$$

The normal vector $\mathbf{n}_1$ can be expressed in the coordinate system F_2 by using E as

$$\mathbf{n}_2 = R\mathbf{n}_1 = R(\mathbf{t} \times \mathbf{x}_1) = RS\mathbf{x}_1 = E\mathbf{x}_1. \tag{31}$$

Denoting

$$\mathbf{n}_2 = [p, q, s]^T, \tag{32}$$

we can write the equation of the plane π in the coordinate system F_2 as

$$px + qy + sz = 0. \tag{33}$$

Assuming that $s \neq 0$, i.e. the epipolar plane does not contain the axis of the second mirror. We can express z as a function of x, y from Eq. (33) and substitute it into the mirror Eq. (3). Assuming $Q = Q_h$ from (11), we obtain the second order polynomial in x, y

$$\begin{aligned}&\big(p^2b_2^2 - s^2a_2^2\big)x^2 + 2pqb_2^2xy + \big(q^2b_2^2 - s^2a_2^2\big)y^2 \\ &\quad - 2spb_2^2e_2x - 2sqb_2^2e_2y + s^2b_2^4 = 0\end{aligned} \tag{34}$$

which is actually a quadratic form of the conic defined by Eq. (28). Parameters a_2, b_2 in Eq. (34) are related to the second mirror, since we are interested in the intersection of the epipolar plane with the second mirror. Consequently, the matrix $A_{\bar{\mathbf{x}}_2}$ from (28) has the form

$$A_{\bar{\mathbf{x}}_2} = \begin{bmatrix} p^2b_2^2 - s^2a_2^2 & pqb_2^2 & -pse_2b_2^2 \\ pqb_2^2 & q^2b_2^2 - s^2a_2^2 & -qse_2b_2^2 \\ -pse_2b_2^2 & -qse_2b_2^2 & s^2b_2^4 \end{bmatrix}. \tag{35}$$

The corresponding point on the second mirror, $\mathbf{x}_2$, lies on the epipolar plane π. Using Eq. (33), the coordinates of $\mathbf{x}_2$ can be expressed as a linear function of $\bar{\mathbf{x}}_2$,

$$\mathbf{x}_2 = \begin{bmatrix} x \\ y \\ \frac{-px-qy}{s} \end{bmatrix} = \begin{bmatrix} 1 & 0 & 0 \\ 0 & 1 & 0 \\ -\frac{p}{s} & -\frac{q}{s} & 0 \end{bmatrix} \bar{\mathbf{x}}_2. \tag{36}$$

It follows from Eq. (18) (for $a = a_2$, $b = b_2$) and Eq. (36) that[3] the relation between $\bar{\mathbf{u}}_2$ and $\bar{\mathbf{x}}_2$ is given by

$$\begin{aligned}&\mathcal{F}_h\big(R_{c2}^T K_2^{-1}\mathbf{u}_2\big) R_{c2}^T K_2^{-1}\mathbf{u}_2 \\ &\quad = \left(\mathbf{x}_2 + \begin{bmatrix} 0 \\ 0 \\ 2e_2 \end{bmatrix}\right) = \begin{bmatrix} 1 & 0 & 0 \\ 0 & 1 & 0 \\ -\frac{p}{s} & -\frac{q}{s} & 2e_2 \end{bmatrix} \bar{\mathbf{x}}_2.\end{aligned} \tag{37}$$

Since $\mathcal{F}_h(R_{c2}^T K_2^{-1}\mathbf{u}_2) \neq 0$ for $s \neq 0$, we can write

$$\begin{aligned}&\bar{\mathbf{x}}_2 \simeq NR_{c2}^T K_2^{-1}\mathbf{u}_2, \quad \text{where} \\ &N = \begin{bmatrix} 1 & 0 & 0 \\ 0 & 1 & 0 \\ \frac{p}{2se_2} & \frac{q}{2se_2} & \frac{1}{2e_2} \end{bmatrix}\end{aligned} \tag{38}$$

and the symbol $\simeq$ denotes "equality up to a nonzero scale". Vector $\bar{\mathbf{x}}_2$ given by Eq. (38) can be substituted into Eq. (28), yielding the desired equation of the epipolar conic in the image plane

$$\mathbf{u}_2^T K_2^{-T} R_{c2} N_2^T A_{\bar{\mathbf{x}}_2} N_2 R_{c2}^T K_2^{-1}\mathbf{u}_2 = 0 \tag{39}$$

and leaving us finally with

$$A_2 = K_2^{-T} R_{c2} B_2 R_{c2}^T K_2^{-1}, \tag{40}$$

where

$$B_2 = N^T A_{\bar{\mathbf{x}}_2} N = \begin{bmatrix} -4s^2a_2^2e_2^2 + p^2b_2^4 & pqb_2^4 & psb_2^2\big(-2e_2^2 + b_2^2\big) \\ pqb_2^4 & -4s^2a_2^2e_2^2 + q^2b_2^4 & qsb_2^2\big(-2e_2^2 + b_2^2\big) \\ psb_2^2\big(-2e_2^2 + b_2^2\big) & qsb_2^2\big(-2e_2^2 + b_2^2\big) & s^2b_2^4 \end{bmatrix} \tag{41}$$

is a nonlinear function of a_2, b_2, and

$$\begin{aligned}[p, q, s]^T = E\Big(&\big[\mathcal{F}_h\big(R_{c1}^T K_1^{-1}\mathbf{u}_1\big) R_{c1}^T K_1^{-1}\mathbf{u}_1\big]^T \\ &- [0, 0, 2e_1]^T\Big)\end{aligned} \tag{42}$$

with $\mathcal{F}_h(R_{c1}^T K_1^{-1}\mathbf{u}_1)$ defined by Eq. (19) for $a = a_1$, $b = b_1$. Equation (39) defines the curve on which the projected corresponding point has to lie. It is, indeed, an equation of a conic as alleged by Eq. (27).

Equation (39) holds true even for $s = 0$ though it was derived for $s \neq 0$. When $s = 0$, the epipolar plane contains the axis of the mirror. It intersects the mirror in hyperbolas which project into lines. Substituting $s = 0$ into Eq. (41) reveals that in this case, B_2 is singular and Eq. (39) describes a line.

Shape of Conics 1. The epipolar conics of a central catadioptric camera with a hyperbolic mirror are ellipses, hyperbolas, parabolas, or lines. The shape depends on the angle between the epipolar plane and the mirror symmetry axis, as well as on the orientation of the perspective camera with respect to the mirror.

Proof: A plane passing through the focal point of a hyperboloid defines a planar intersection conic. The shape of the conic depends on the angle between the plane and the rotation axis of the hyperboloid. In particular, it is a hyperbola for the zero angle between the plane and the axis. The conic is projected into the image by a homography which maps conics to conics. The intersection conic is projected into the image as a line if the epipolar plane contains the symmetry axis of the mirror. The line can be at infinity if the image plane is parallel to the plane formed by rays that project the intersection conic into the image plane. That can happen only if the image plane is parallel to the epipolar plane. The classification of the conic can be based on the matrix A_2 defined by (40). □

However, the matrix A_2 is very difficult to analyze analytically. In the Appendix, we provide an analytical analysis of $A_{\tilde{\mathbf{x}}_2}$ from (35), which is sufficient for the most common case, i.e. when the image plane is perpendicular to the mirror axis.

4.2. Elliptic Mirror

The derivation is performed in the same manner as that for the hyperbolic mirror. The matrix Q from (3) equals to Q_e from (20). Since the mirror equation differs we end up with different conic matrices. The matrix $A_{\tilde{\mathbf{x}}_2}$ from (35) changes to

$$A_{\tilde{\mathbf{x}}_2} = \begin{bmatrix} p^2b^2 + s^2a^2 & pqb^2 & -pseb^2 \\ pqb^2 & q^2b^2 + s^2a^2 & -qseb^2 \\ -pseb^2 & -qseb^2 & -s^2b^4 \end{bmatrix}. \tag{43}$$

The final expression for A_2, $A_2 = K_2^{-T} R_{c2} B_2 R_{c2}^T K_2^{-1}$, is the same, only B_2 changes to

$$B_2 = N^T A_{\mathbf{x}_2} N = \begin{bmatrix} 4s^2a^2e^2 - p^2b^4 & -pqb^4 & -psb^2(2e^2 + b^2) \\ -pqb^4 & 4s^2a^2e^2 - q^2b^4 & -qsb^2(2e^2 + b^2) \\ -psb^2(2e^2 + b^2) & -qsb^2(2e^2 + b^2) & -s^2b^4 \end{bmatrix} \tag{44}$$

Shape of Conics 2. Epipolar conics for an elliptic mirror are ellipses or lines.

Proof: A plane passing through the focal point of an ellipsoid defines a planar intersection ellipse. The intersection ellipse is projected into the image by a homography that maps conics to conics. If an epipolar plane contains both focal points, then the intersection conic is projected to a line in the image. The line can be at infinity if the image plane is parallel with the plane formed by the rays that project the intersection conic into the image plane. This can happen only if the image plane is parallel to the epipolar plane. Epipolar conics are projected to ellipses in all other cases, which can easily be verified by showing that the first subdeterminant of (43) is always positive. □

4.3. Parabolic Mirror

The derivation of $A_2(E, \mathbf{u}_1)$ from Eq. (27) for a parabolic mirror is the same as it was for the hyperbolic mirror as far as Eq. (33). Then, the shape of the parabolic mirror is to be considered. Assuming $s \neq 0$ and $Q = Q_p$ from (7), we substitute z from Eq. (33) into the equation for a parabolic mirror (3) and obtain the equation of epipolar conics

$$sx^2 + 2b_2px + sy^2 + 2b_2qy - sb_2^2 = 0, \tag{45}$$

where b_2 is the mirror parameter and p, q, s are defined by Eq. (32). Matrix $A_{\tilde{\mathbf{x}}_2}$ from Eq. (28) becomes

$$A_{\tilde{\mathbf{x}}_2} = \begin{bmatrix} s & 0 & b_2p \\ 0 & s & b_2q \\ b_2p & b_2q & -b_2^2s \end{bmatrix}, \tag{46}$$

with

$$\begin{bmatrix} p \\ q \\ s \end{bmatrix} = E \begin{bmatrix} x \\ y \\ \frac{x^2+y^2}{2b_1} \end{bmatrix}, \quad \begin{bmatrix} x \\ y \\ 1 \end{bmatrix} = R_{c1}^T K_1^{-1} \mathbf{u}_1 \qquad (47)$$

following from Eqs. (10) and (31).

It follows from Eq. (10) that $\bar{\mathbf{x}}_2$ is related to $\mathbf{u}_2$ by a linear transformation (compare to Eq. (38))

$$\bar{\mathbf{x}}_2 = R_{c2}^T K_2^{-1} \mathbf{u}_2. \qquad (48)$$

Substituting (48) and (46) into (28) yields the fundamental epipolar constraint for the parabolic mirror

$$\mathbf{u}_2^T K_2^{-T} R_{c2} A_{\bar{\mathbf{x}}_2} R_{c2}^T K_2^{-1} \mathbf{u}_2 = 0, \qquad (49)$$

and therefore

$$A_2 = K_2^{-T} R_{c2} A_{\bar{\mathbf{x}}_2} R_{c2}^T K_2^{-1}, \qquad (50)$$

where $A_{\bar{\mathbf{x}}_2}$ is defined by Eq. (46).

Shape of Conics 3. Epipolar conics for a parabolic mirror are ellipses, lines, or a point at infinity. In a physical image, only ellipses or lines can appear. The shape depends on the angle between the epipolar plane and the mirror symmetry axis as well as the angle between the image plane and the axis.

Proof: The epipolar plane intersects a parabolic mirror in an intersection conic. It is a parabola if the angle between the epipolar plane and the axis is zero. Otherwise, it is an ellipse.

Let the intersection conic be an ellipse. In the Appendix it is shown that the intersection ellipse always projects into a circle in the xy plane of the coordinate system F. Therefore, the parallel rays which project the ellipse into the image form a cylinder which has a circular cross-section. The conic in the image plane is the result from the intersection of the cylinder with the image plane. A plane and a cylinder always intersect. The intersection is an ellipse if the angle between the plane and the axis of the cylinder is not zero. If it is zero, then the intersection can be either a line, a pair of lines, or a point at infinity on the axis. It is a single line or a pair of lines if the image plane has a finite intersection with the cylinder. It is a point at infinity if there is no finite intersection of the plane and the cylinder.

Let the intersection conic be a parabola. The parallel rays which project the parabola into the image form a plane. The conic in the image is the result of from the intersection of two planes which forms a line. If the planes are parallel, then the line is at infinity. There is no image conic if the planes are identical. □

5. Experiments

To illustrate the theory and provide examples of images and epipolar conics, experiments with real central catadioptric cameras with a parabolic and hyperbolic mirror are presented. Experiments with a synthetic elliptical mirror were also performed but are not presented here because of the similarity with the hyperbolic case. Epipolar geometry was estimated from more than 8 corresponding points, typically from 20–30 points. Correspondences were selected manually using the RecX[4] tool (Buriánek, 1998). The essential matrix was estimated by solving the set of homogeneous equations

$$\mathbf{x}_2^T E \mathbf{x}_1 = 0.$$

A standard total least square (TLSQ) solution by singular value decomposition (SVD) (Van Huffel and Vandewalle, 1991) with a simple point normalization (Pajdla et al., 2001) was used. Robustness of the method against outliers is not of interest here, the interested reader is referred to Svoboda (2000).

Recently, some elaborate methods for the estimation of E appeared. Chang and Hebert (2000) suggested to use the Levenberg-Marquard minimization for the estimation of motion parameters $\mathbf{t}$, R. Another exhaustive minimization procedure was proposed by Kang (2000). He seeks the calibration parameters together with the Essential matrix using Nelder-Mead simplex search algorithm.

The calibration parameters of catadioptric cameras have to be known a priori or estimated from images for computing epipolar geometry. Some calibration methods appeared recently. Geyer and Daniilidis (1999) use a large dot pattern or points along lines. Their catadioptric camera with a parabolic mirror can be calibrated on the basis of just one image. Kang (2000) does not use any special calibration pattern, he proposes a self-calibration method from multiple images. In fact, we do not need any calibration methods here. We designed the hyperbolic mirror and the it was assembled with a pre-calibrated camera in order to fulfill the requirements, see Fig. 7. The perspective camera was calibrated using (Pajdla, 1995). The parabolic mirror was purchased from Cyclovision together with an orthographic lens.

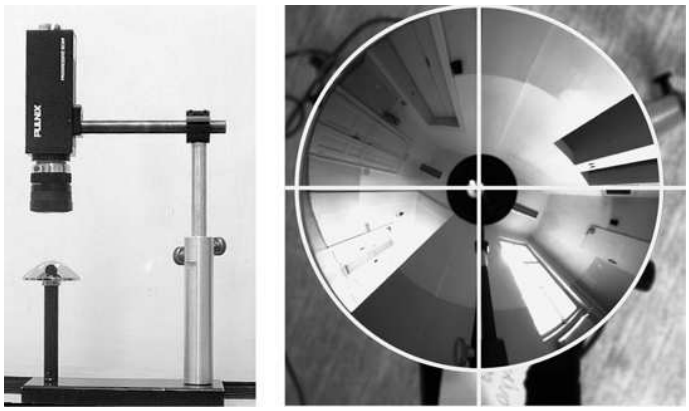

Figure 7. The assembly of our central catadioptric camera with a hyperbolic mirror. The calibration pattern was computed from the known camera and mirror parameters. The mutual position of the camera and the mirror was tuned until the pattern fits the image of the mirror.

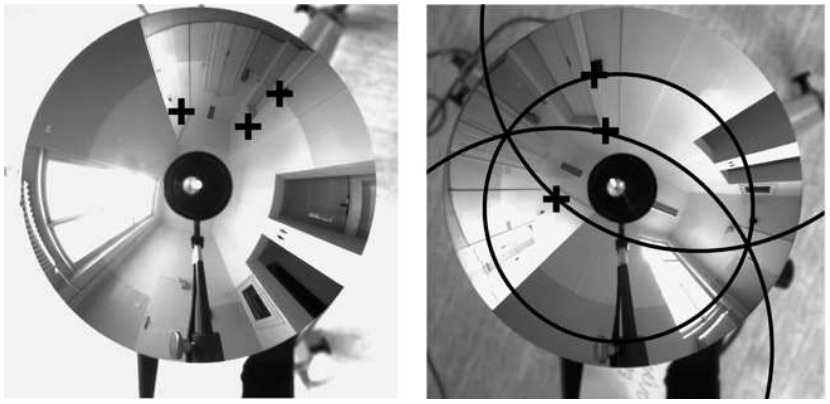

Figure 8. Illustration of the epipolar geometry of a central catadioptric camera with a hyperbolic mirror. Three points are chosen in the left-hand image. Their corresponding epipolar conics are shown in the right-hand image. The conics intersect in two epipoles and pass through the corresponding points.

The mirror parameter a was computed from the dimensions of the mirror, the principal point of the camera was assumed to be the center of the projected mirror rim. The projection of the mirror rim was found by fitting a circle to the points on the rim. The points were extracted manually from the images.

5.1. Hyperbolic Mirror

A set of experiments was carried out with a hyperbolic mirror, having a 60 mm diameter parameters $a = 28.1$ mm and $b = 23.4$ mm. The mirror was manufactured by Neovision.[5] A Pulnix digital camera with 1024×1024 pixel resolution was used. The arrangement was such that the Pulnix camera was above and aimed at the mirror placed below, the setup is shown in Fig. 7. The central catadioptric camera was placed on a tripod approximately one meter above the floor and it moved along a corridor. Figure 8 shows an example of the epipolar geometry between a pair of images obtained by this camera. Three corresponding points are marked on the left-hand and on the right-hand image. There are three epipolar conics shown in the right image which correctly pass through the corresponding points. The conics intersect at the two epipoles.

5.2. Parabolic Mirror

A commercially available central catadioptric camera with a parabolic mirror was purchased from

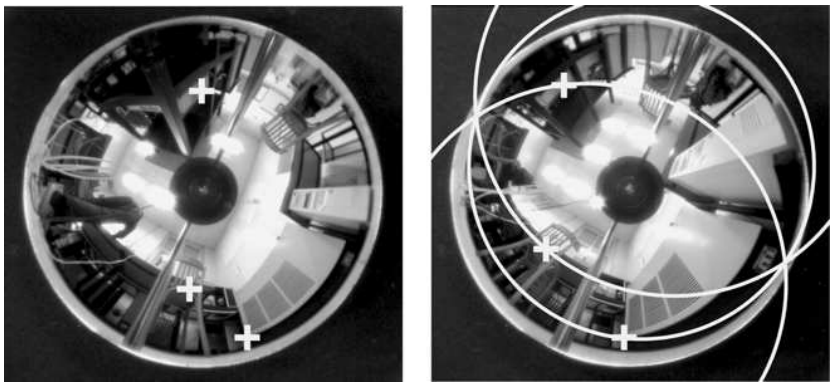

Figure 9. Illustration of the epipolar geometry of a central panoramic catadioptric camera with a parabolic mirror. Three points are chosen in the left-hand image. Their corresponding epipolar conics are shown in the right-hand image. The conics intersect at the two epipoles and pass through the corresponding points.

Cyclovision.[6] The orthographic camera is mounted above the parabolic mirror and it looks in the top-down direction. The whole sensor was moved on the floor in a room sized approximately $6 \times 6 \times 3$ meters. Figure 9 shows an example of the epipolar geometry between a pair of images. Three corresponding points are marked in the left-hand and in the right-hand image. There are three epipolar conics shown in the right image which pass through the corresponding points. The conics intersect again at the two epipoles.

6. Conclusion

A complete characterization of epipolar geometry of a pair of central catadioptric cameras was presented. We have shown that epipolar curves are (i) general conics for a hyperbolic camera; (ii) ellipses or lines for the elliptic and parabolic cameras. The shape of conics depends on the position of a 3D point, on the displacement of the cameras, and on the parameters of the mirrors. Epipolar curves intersect at two epipoles except when the displacement of the cameras is a translation along the common axis of the mirrors. The epipolar constraint can be applied for any displacement of panoramic cameras with a nonzero translation.

Appendix—Shape of Conics

Hyperbolic Mirror

The key features are the determinant $\Delta = \det(A_{\bar{\mathbf{x}}_2})$, (35), and the sub-determinant of the sub-matrix composed from the first two rows and the first the two columns (Hazewinkel, 1995). The sub-determinant is denoted by δ. Suppose a non-degenerate conic, i.e. $\Delta \neq 0$, holds. The shape of the conic depends on δ and it can be

$$\begin{array}{ll} \text{an ellipse} & \text{if } \delta > 0, \\ \text{a hyperbola} & \text{if } \delta < 0, \\ \text{a parabola} & \text{if } \delta = 0. \end{array}$$

Note that the normal $\mathbf{n}$ of the epipolar plane (31, 32) is normalized, i.e. $p^2 + q^2 + s^2 = 1$. The first sub-determinant δ of matrix $A_{\bar{\mathbf{x}}_2}$, Eq. (35), is given by the equation

$$\delta = s^2a^2(s^2a^2 - p^2b^2 - q^2b^2).$$

Let us assume that the conic is an *ellipse*. Then,

$$s^2a^2 - b^2(p^2 + q^2) > 0$$
$$s^2 > \frac{b^2}{a^2 + b^2}.$$

In the same way it can be derived that the conic is a *hyperbola* if

$$s^2 < \frac{b^2}{a^2 + b^2}.$$

and a *parabola* if

$$s^2 = \frac{b^2}{a^2 + b^2}.$$

The shape of a conic also depends on mirror parameters and on the angle between the epipolar plane and the axis

of the mirror. The conic is degenerate if the matrix $A_{\bar{\mathbf{x}}_2}$ is singular, i.e. $\Delta = 0$. It can be shown that the matrix $A_{\bar{\mathbf{x}}_2}$ is singular if $s = 0$. We have already shown that by substituting $s = 0$ into (41) and (39) the conic becomes a radial line in that case.

Moreover, the actual equation of the conic also depends on how a coordinate system is chosen in the image. However, as a choice of a coordinate system can, at most, induce only an affine transformation, the type of a conic will not be altered by different choices of the coordinate system.

Parabolic Mirror

The quadratic form (45) can be rewritten as

$$x^2 + \frac{2ap}{s}x + y^2 + \frac{2aq}{s}y - a^2 = 0. \qquad (51)$$

Conversion to the total squares form yields

$$\left(x + \frac{ap}{s}\right)^2 + \left(y + \frac{aq}{s}\right)^2 - \left(a^2 + \frac{a^2p^2}{s^2} + \frac{a^2q^2}{s^2}\right) = 0,$$

and further

$$\left(x + \frac{ap}{s}\right)^2 + \left(y + \frac{aq}{s}\right)^2 - \frac{a^2}{s^2}\|\mathbf{n}_2\|^2 = 0.$$

Because $\mathbf{n}_2$ is a normal vector, $\|\mathbf{n}_2\| = 1$, the above equation can be rewritten as

$$\left(x + \frac{ap}{s}\right)^2 + \left(y + \frac{aq}{s}\right)^2 = \frac{a^2}{s^2}. \qquad (52)$$

Epipolar conics for the combination of an orthographic camera and a parabolic mirror form cylinders with a circular section and with the axis being the same as the axis of the mirror.

Notes

1. For a parabola oriented vertically and opening upwards, the vertex is the point where the curve reaches a minimum.
2. If the twofold projection is allowed, the right λ is chosen according to the position of the direct projection of X. It is the negative λ which is the right one for the points outside the shaded zone, because point $\mathbf{x}$ lies on the opposite side of F than point X.
3. We use $\mathbf{t}_c = [0, 0, -2e_2]^T$ since the center C has to coincide with the focal point F'.
4. `http://cmp.felk.cvut.cz/cmp/recx`.
5. `http://www.neovision.cz/prods/panoramic/`.
6. `http://www.cyclovision.com`, now `http://www.remotereality.com/`.

References

Baker, S. and Nayar, S.K. 1999. A theory of single-viewpoint catadioptric image formation. *International Journal of Computer Vision*, 35(2):1–22.

Brodsky, T., Fermueller, C., and Aloimonos, Y. 1998. Directions of motion fields are hardly ever ambiguous. *International Journal of Computer Vision*, 26(1):5–24.

Buriánek, J. 1998. Korespondence pro virtualní kameru. Master's Thesis, Czech Technical University, Center for Machine Perception, Department of Control Engineering, Czech Republic (in Czech).

Chang, P. and Hebert, M. 2000. Omni-directional structure from motion. In *IEEE Workshop on Omnidirectional Vision*, K. Daniilidis (Ed.). IEEE Computer Society Press: Los Alamitos, CA, pp. 127–133.

Descartes, R. and Smith, D.T. 1954. *The Geometry of René Descartes*. Dover Publ.: New York. Originally published in Discours de la Methode, 1637.

Faugeras, O. 1993. *3-D Computer Vision, A Geometric Viewpoint*. MIT Press: Cambridge, MA.

Geyer, C. and Daniilidis, K. 1999. Catadioptric camera calibration. In *The 7th International Conference on Computer Vision*, Kerkyra, Greece, vol. I, IEEE Computer Society Press: Los Alamitos, CA, pp. 398–404.

Gluckman, J. and Nayar, S.K. 1998. Ego-motion and omnidirectional cameras. In *The Sixth International Conference on Computer Vision*, Bombay, India, S. Chandran and U. Desai (Eds.). Narosa Publishing House, pp. 999–1005.

Hartley, R. and Zisserman, A. 2000. *Multiple View Geometry in Computer Vision*. Cambridge University Press: Cambridge, UK.

Hazewinkel, M. (Ed.). 1995. *Encyclopaedia of Mathematics*. Kluwer Academic Publishers: Dordrecht, MA.

Hecht, E. 1975. *Optics*, Schaum Outline Series. McGraw-Hill: New York.

Kang, S.B. 2000. Catadioptric self-calibration. In *International Conference on Computer Vision and Pattern Recognition*, vol. I, IEEE Computer Society Press: Los Alamitos, CA, pp. 201–207.

Nayar, S. and Peri, V. 1999. Folded catadioptric cameras. In *Conference on Computer Vision and Pattern Recognition*, Fort Collins, Colorado, vol. II, IEEE Computer Society Press: Los Alamitos, CA, pp. 217–223.

Nene, S.A. and Nayar, S.K. 1998. Stereo with mirrors. In *The Sixth International Conference on Computer Vision,* Bombay, India, S. Chandran and U. Desai (Eds.). Narosa Publishing House, pp. 1087–1094.

Pajdla, T. 1995. BCRF—Binary Illumination Coded Range Finder: Reimplementation. ESAT MI2 Technical Report Nr. KUL/ESAT/MI2/9502, Katholieke Universiteit Leuven, Belgium.

Pajdla, T., Svoboda, T., and Hlaváč, V. 2001. Epipolar geometry of central panoramic cameras. In *Panoramic Vision: Sensors, Theory, and Applications*, R. Benosman and S.B. Kang (Eds.). Springer Verlag: New York, pp. 85–114.

Semple, J.G. and Kneebone, G.T. 1998. *Algebraic Projective Geometry*, 4th edn. Oxford Classic Texts in the Physical Sciences, Clarendon Press: Oxford, USA.

Southwell, D., Basu, A., Fiala, M., and Reyda, J. 1996. Panoramic stereo. In *13th International Conference on Pattern Recognition*, Vienna, Austria, vol. A, IEEE Computer Society Press: Los Alamitos, CA, pp. 378–382.

Svoboda, T. 2000. Central panoramic cameras design, geometry, egomotion. Ph.D. Thesis, Center for Machine Perception, Czech Technical University, Prague, Czech Republic.

Svoboda, T. and Pajdla, T. 2000. Panoramic cameras for 3D computation. In *Proceedings of the Czech Pattern Recognition Workshop*, Prague, Czech Republic, T. Svoboda (Ed.). Czech Society for Pattern Recognition, pp. 63–70. Also available at http://cmp.felk.cvut.cz/~svoboda/Publications/svobCPRW2000.html.

Svoboda, T., Pajdla, T., and Hlaváč, V. 1998a. Epipolar geometry for panoramic cameras. In *The Fifth European Conference on Computer Vision,* Freiburg, Germany, H. Burkhardt and N. Bernd (Eds.). Springer: Berlin, pp. 218–232.

Svoboda, T., Pajdla, T., and Hlaváč, V. 1998b. Motion estimation using central panoramic cameras. In *IEEE International Conference on Intelligent Vehicles*, Stuttgart, Germany, S. Hahn (Ed.). Causal Productions, pp. 335–340.

Van Huffel, S. and Vandewalle, J. 1991. *The Total Least Squares Problem: Computational Aspects and Analysis*, vol. 9 of *Frontiers in Applied Mathematics*. Society for Industrial and Applied Mathematics: Philadelphia.

Yagi, Y. 1999. Omnidirectional sensing and its applications. *IEICE Transactions on Information and Systems*, E82-D(3):568–579.

Yamazawa, K., Yagi, Y., and Yachida, M. 1995. Obstacle detection with omnidirectional image sensor hyperomni vision. In *IEEE International Conference on Robotics and Automation 1995*, pp. 1062–1067.